

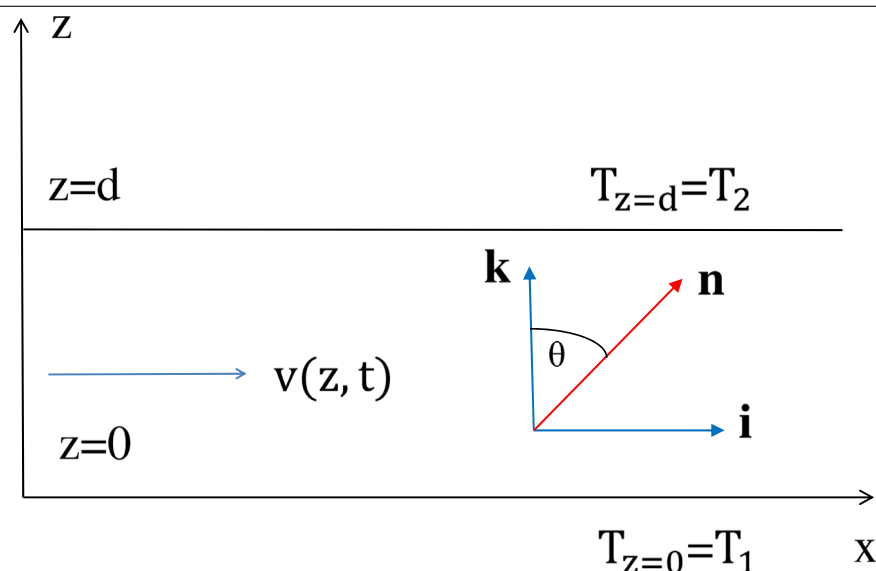


Research paper

Comprehensive analysis of compressible and incompressible nematic flow caused by thermomechanical force

Izabela Śliwa^a, Pavel V. Maslennikov^b, Sergey V. Pasechnik^c, Alex V. Zakharov^{d,e} *^a Poznan University of Economics and Business, Al. Niepodległości 10, 61-875 Poznan, Poland^b Immanuel Kant Baltic Federal University, Kaliningrad 236040, Str. Universitetskaya 2, Russia^c Russian Technological University (MIREA), Moscow, 119454, Russia^d Institute for Problems in Mechanical Engineering of the Russian Academy of Science (IPME RAS), Bolshoy pr. V.O., 61, St-Petersburg, 199178, Russia^e National Research University Higher School of Economics, St-Petersburg, 194100, Russia

GRAPHICAL ABSTRACT



ARTICLE INFO

Keywords:

Liquid crystals

Hydrodynamics of anisotropic systems

Compressible nematics

ABSTRACT

A numerical study of the effect of thermomechanical force on dissipation processes in a micro-sized compressible and incompressible hybrid aligned nematics has been carried out. Calculations have shown that under the effect of a temperature gradient ∇T , a hybrid aligned compressible and incompressible nematic samples settle down to the stationary flow \mathbf{v} regimes, and the thermomechanical force strongly influences the directions and magnitudes of \mathbf{v} . A small quantitative difference was found in the equilibrium distribution of the horizontal velocity component for both compressible and incompressible nematic flow caused by the same ∇T , which is set up across the micro-sized hybrid aligned nematic channel.

* Corresponding author at: Institute for Problems in Mechanical Engineering of the Russian Academy of Science (IPME RAS), Bolshoy pr. V.O., 61, St-Petersburg, 199178, Russia.

E-mail addresses: izabela.sliwa@ue.poznan.pl (I. Śliwa), pashamaslennikov@mail.ru (P.V. Maslennikov), s-p-a-s-m@mail.ru (S.V. Pasechnik), alexandre.zakharov@yahoo.ca (A.V. Zakharov).

URL: <https://www.ipme.ru> (A.V. Zakharov).

<https://doi.org/10.1016/j.cplett.2025.142528>

Received 8 September 2025; Received in revised form 2 November 2025; Accepted 7 November 2025

Available online 8 November 2025

0009-2614/© 2025 Elsevier B.V. All rights reserved, including those for text and data mining, AI training, and similar technologies.

1. Introduction

A liquid crystal (LC) drop of micro sized volume are extremely sensitive to both the temperature gradient ∇T and boundary conditions. Consequently, these factors, can influence the nature of hydrodynamic flow \mathbf{v} in micro- or nanosized LC channels. One of the nonmechanical method for producing flow in a nematic microfluidic channel is based on the coupling between the temperature ∇T and the director field $\nabla \hat{\mathbf{n}}$ gradients. The problem of motion associated with an ultra-small (a few microliters) nematic drops, under the influence of the temperature gradient has drawn considerable attention [1–13]. The temperature gradient ∇T can be generated either by a laser beam focused inside the nematic microvolume and at the nematic channel boundary, or by inhomogeneous heating of the nematic channel or capillary boundaries. In turn, the director field $\nabla \hat{\mathbf{n}}$ gradient across the nematic micro volume can be formed by hybrid alignment of the LC volume on the bounding surfaces, for instance, homeotropic alignment on the upper and homogeneous on the lower bounding surfaces. The possibility of using a nearly infrared laser as a microfluidic heat source has been addressed by several groups [5–10,12]. Lasers provide the opportunity of precise tunable spatial and temporal properties of optical irradiation, providing controllable heating of the LC system. Coupling between ∇T and $\nabla \hat{\mathbf{n}}$, which is responsible for the excitation of an additional force in the LC phase called the thermomechanical force [2] (TMF)

$$F_i = \partial \sigma_{ji}^{\text{tm}} / \partial x_j, \quad (1)$$

where $\sigma_{ji}^{\text{tm}} = \xi_{ijklp} (\nabla_k T) (\nabla_l n_p)$ is the thermomechanical stress tensor, which is one of the main factors that distinguish the LC system from isotropic molecular liquids. Here ξ_{ijklp} is the thermomechanical coupling tensor [2]. The magnitude of the hydrodynamic flow \mathbf{v} excited by ∇T in a hybrid aligned nematic (HAN) volume is proportional to the tangential component of the thermomechanical stress tensor (TMST) σ_{zx}^{tm} and has the form

$$v \sim \frac{d}{\eta} \sigma_{zx}^{\text{tm}}, \quad (2)$$

where d and η are the thickness and viscosity of the liquid crystal material, respectively. The direction of \mathbf{v} is influenced by both the direction of the heat flux $\mathbf{q} = -T \frac{\delta \mathcal{R}}{\delta \nabla T}$ and the character of the preferred anchoring of the director $\hat{\mathbf{n}}$ to the restricted surfaces [4,11,13]. Here \mathcal{R} is the Rayleigh dissipation function of LC system. It has been shown that the main factor influencing the magnitude and direction of the excited fluid flow is the coupling between ∇T and $\hat{\mathbf{n}}$. This thermomechanical force is a key factor responsible for the correct description of dissipation processes and the excitation of hydrodynamic flow in micro-sized LC channels. Thus, the development of physically controlled systems is required to accurately study the thermomechanical force.

Recently, based on a nonlinear extension of the Ericksen–Leslie theory [14,15] with taking into account the entropy balance equation [16], a theoretical study of heating in a micro-sized hybrid aligned compressible nematic (HACN) volume caused by inhomogeneous heating of the nematic volume boundaries has been carried out [13]. Calculations showed that under the effect of ∇T , the HACN sample settles down to a stationary flow regime with both horizontal u and vertical w components of velocity \mathbf{v} , and direction and magnitude of \mathbf{v} is strongly effected by the direction of ∇T .

However, given that the thickness of the micro-sized nematic channel is on the order of several tens of micrometers, changes in the LC density across this volume are insignificant, and with high accuracy it can be assumed that the micro-volume is incompressible. Thus, the comparative analysis of the relaxation of hydrodynamic flow caused by TMF in both compressible and incompressible HAN microvolume under the effect of ∇T is useful both from an academic and practical point of view, and is also an essential part of knowledge in the field of soft-matter science.

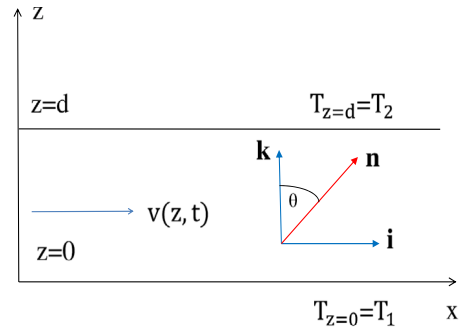


Fig. 1. The coordinate system used for theoretical analysis. The x -axis is taken as being parallel to the director directions on the upper surface, $\theta(z, t)$ is the angle between the director $\hat{\mathbf{n}}$ and the unit vector $\hat{\mathbf{k}}$, respectively.

The outline of this paper is as follow: the system of hydrodynamic equations describing both director motion and fluid flow of a compressible LC phase confined between two bounding surfaces, with accounting for the heat conduction, caused by heating from below, is given in Section 2. Numerical investigation the effect of thermomechanical force on relaxation processes in compressible HAN microvolume is given in Section 3. A comparative analysis of the relaxation regimes of the formation of hydrodynamic flow caused by the thermomechanical force in both compressible and incompressible HAN microvolume is given in Section 4. Conclusions are summarized in Section 5.

2. Basic hydrodynamic equations

The main aim of our numerical study is to clarify the role of the tangential component of the thermomechanical stress tensor σ_{zx}^{tm} in the excitation of hydrodynamic flow in such micro-sized compressible and incompressible HAN system, where the gradient of director field $\nabla \hat{\mathbf{n}}$ is set up due to different alignment of the director field $\hat{\mathbf{n}}$ on the bounding surfaces (see Fig. 1).

We would like to focus on the numerical study of the evolution of temperature T , density ρ , velocity \mathbf{v} and director $\hat{\mathbf{n}}$ distributions, which are produced in a two-dimensional (2D) micro-sized compressible HAN channel under the effect of a temperature gradient ∇T (Fig. 1). The hydrodynamic model used in the numerical study is based on the Ericksen–Leslie theory [14,15], taking into account the entropy balance equation [10] and the equation of state, and was previously formulated in [16]. Consider the 2D compressible HAN volume, which is bounded by two infinitely long boundaries at a distance of d on a scale of the order of tens micrometers and is initially at rest. Assuming that the temperature gradient ∇T is established due to different heating of the bounding surfaces, we will consider the case when the upper surface is hotter than the lower one, and the boundary condition for the dimensionless temperature field must satisfy

$$\chi_{z=1} = \chi_{\text{up}} = \chi_2, \quad \chi_{z=0} = \chi_{\text{lw}} = \chi_1, \quad (3)$$

$$\chi_2 > \chi_1 \text{ (CASE I),}$$

where $\chi(z) = T(z)/T_{\text{NI}}$ is the dimensionless temperature, T_{NI} is the nematic-isotropic transition temperature, $\chi_1 = T_1/T_{\text{NI}}$ and $\chi_2 = T_2/T_{\text{NI}}$ are the dimensionless values of temperature on lower and upper surfaces, respectively. Here $\bar{z} = z/d$ is the dimensionless distance away from the lower solid surface, and the overbar in the space variable z has been eliminated.

Thus, the solid surfaces are kept at different temperatures, and the compressible HAN volume is exposed to the temperature gradient $\nabla \chi$ directed parallel to the unit vector $\hat{\mathbf{k}}$ directed from the lower substrate to the upper one in the direction of z . Moreover, we can assume that the temperature gradient changes only in the z direction, and we can assume that the components of the director $\hat{\mathbf{n}} = n_x(z, \tau)\hat{\mathbf{i}} + n_z(z, \tau)\hat{\mathbf{k}} =$

$\sin \theta(z, \tau) \hat{\mathbf{i}} + \cos \theta(z, \tau) \hat{\mathbf{k}}$ field, as well as other physical quantities, depends only on the coordinate z and time τ . Here θ denotes the polar angle, i.e., the angle between the direction of the director $\hat{\mathbf{n}}$ and the unit vector $\hat{\mathbf{k}}$, while the unit vector $\hat{\mathbf{i}}$ is directed parallel to the lower substrate, and $\hat{\mathbf{j}} = \hat{\mathbf{k}} \times \hat{\mathbf{i}}$, respectively. Here $\tau = (K_{10}/\gamma_{10}d^2)t$ is the dimensionless time, K_{10} and γ_{10} are the highest values for elastic and rotational viscosity coefficients, respectively. If the HAN volume, with the homeotropic aligning of the director field $\hat{\mathbf{n}}_{z=0} \parallel \hat{\mathbf{k}}$ on the lower, and planar $\hat{\mathbf{n}}_{z=1} \parallel \hat{\mathbf{i}}$, on the upper bounding surfaces is heated from below or above, due to the coupling between $\nabla \chi$ and $\nabla \hat{\mathbf{n}}$ in this LC volume, the hydrodynamic flow $\mathbf{v}(z, \tau) = v_x(z, \tau) \hat{\mathbf{i}} + v_z(z, \tau) \hat{\mathbf{k}} = u(z, \tau) \hat{\mathbf{i}} + w(z, \tau) \hat{\mathbf{k}}$ is exited.

The 2D compressible HAN film confined between two solid surfaces suggests that

$$\theta(z)_{z=0} = 0, \quad \theta(z)_{z=1} = \frac{\pi}{2}, \quad (4)$$

and its initial orientation is perturbed to be tilted with respect to the interface, with

$$\theta(z, \tau = 0) = \frac{\pi}{2}, \quad (5)$$

and then allowed to relax to its equilibrium value $\theta_{\text{eq}}(z)$. In turn, the velocity on these surfaces has satisfy the no-slip boundary condition

$$\begin{aligned} u(z)_{z=0} &= 0, \quad u(z)_{z=1} = 0, \\ w(z)_{z=0} &= 0, \quad w(z)_{z=1} = 0. \end{aligned} \quad (6)$$

Now, the reorientation of director field $\hat{\mathbf{n}}$ in the HAN film, confined between two solid surfaces, under the effect of the temperature gradient $\nabla \chi$, when the relaxation regime is governed by viscous, elastic, and thermomechanical forces with accounting for hydrodynamic flow \mathbf{v} , can be obtained by solving a system consisting of mass, torque, momentum, and entropy balance equations.

Since our main aim is to clarify the role of the tangential component of the thermomechanical stress tensor σ_{zx}^{tm} in the excitation of hydrodynamic flow in microscaled compressible and incompressible HAN system, when the gradient of director field $\nabla \hat{\mathbf{n}}$ is set up due to different alignment of the director field $\hat{\mathbf{n}}$ on the bounding surfaces, we will use the balance equations of dimensionless mass, torque, momentum and entropy in form in which they are presented in [13]. First of all, the condition of dimensionless compressibility, in the form of Boussinesq approximation [13], can be rewritten as

$$\left(\frac{1}{\delta_1} + \chi_1 - \chi \right) w_{,z} - \chi_{,\tau} - \chi_{,z} w = 0, \quad (7)$$

where $\delta_1 = T_{\text{NI}} \alpha$ is the parameter of LC system, α is the volume expansion coefficient, $w_{,z} = \partial w(z, \tau) / \partial z$, $\chi_{,\tau} = \partial \chi(z, \tau) / \partial \tau$, while $\bar{w} = \frac{\gamma_{10} d^2}{K_{10}} w$ is the vertical dimensionless component of velocity, respectively. Note that the overbar in the velocity component w has been eliminated. In turn, the dimensionless torque balance equation can be written as (see Ref. [13])

$$\gamma_1(\chi) \theta_{,\tau} = \mathcal{A}(\theta) u_{,z} + (\mathcal{G}(\theta) \theta_{,z})_{,z} - \frac{1}{2} \mathcal{G}_{,\theta}(\theta) \theta_{,z}^2 - \delta_2 \chi_{,z} \theta_{,z} \kappa(\theta), \quad (8)$$

where $\bar{\gamma}_1(\chi) = \gamma_1(\chi) / \gamma_{10}$ is the dimensionless RVC, $u_{,z} = \partial u(z, \tau) / \partial z$, $\mathcal{A}(\theta) = \bar{\mathcal{A}}(\theta) / \gamma_{10} = \frac{1}{2} (\gamma_1(\chi) - \gamma_2(\chi) \cos 2\theta) / \gamma_{10}$, $\mathcal{G}(\theta) = (K_1(\chi) \sin^2 \theta + K_3(\chi) \cos^2 \theta) / K_{10}$, $\mathcal{G}_{,\theta}(\theta)$ is the derivative of $\mathcal{G}(\theta)$ with respect to θ , $\kappa(\theta) = \frac{1}{2} + \sin^2 \theta$, and $\delta_2 = \xi T_{\text{NI}} / K_{10}$ is the parameter of the system, respectively. Here $\xi \sim 10^{-12}$ J/m K is the thermomechanical constant [2], K_1 and K_3 are the splay and bend elastic coefficients, K_{10} , K_{30} and γ_{10} are the highest values for elastic and rotational viscosity coefficients, respectively. In the last equation all overbars have been (and will be) eliminated as well as in the following equations. In the case of compressible fluid the dimensionless momentum balance equation reduces to (see Ref. [13])

$$\delta_3 \left[(1 - \delta_1(\chi - \chi_1)) u \right]_{,\tau} =$$

$$\left[h(\theta) u_{,z} - \mathcal{A}(\theta) \theta_{,\tau} - \delta_2 \chi_{,z} \theta_{,z} \sin^2 \theta + \frac{\beta_0}{6} w_{,z} \sin 2\theta \right]_{,z}, \quad (9)$$

and

$$\begin{aligned} \delta_3 \left[(1 - \delta_1(\chi - \chi_1)) w \right]_{,\tau} = \\ \left[\frac{\bar{\beta}_0}{6} \left(u_{,z} \sin 2\theta + \frac{2}{3} w_{,z} \right) + \zeta_v w_{,z} - \frac{\delta_2}{4} \chi_{,z} \theta_{,z} \sin 2\theta - \mathcal{G}(\theta) \theta_{,z}^2 \right]_{,z}, \end{aligned} \quad (10)$$

respectively. Here $h(\theta) = \alpha_1(\chi) \sin^2 \theta \cos^2 \theta - \mathcal{A}(\theta) \theta_{,\tau} u_{,z} + \frac{1}{4} \alpha_4(\chi) + g(\theta)$, $g(\theta) = \frac{1}{2} (\alpha_6(\chi) \sin^2 \theta + \alpha_5(\chi) \cos^2 \theta)$, $\beta_0 = \alpha_1 + \alpha_5 + \alpha_6 + \frac{3}{2} \alpha_4$, $\alpha_i(\chi)$ ($i = 1, \dots, 6$) are the temperature dependent six Leslie coefficients, $\bar{\beta}_0 = \beta_0 / \gamma_{10}$, $\bar{h}(\theta) = h(\theta) / \gamma_{10}$, ζ_v is the volume viscosity, and $\delta_3 = \rho_0 K_{10} / \gamma_{10}^2$ is an additional parameter of the LC system, respectively. The overbar in $\bar{h}(\theta)$ and $\bar{\beta}_0$ have been eliminated. In turn, the dimensionless temperature field $\chi(z, \tau)$ satisfies the heat conduction equation (see Ref. [13])

$$\begin{aligned} \delta_4 \left[(1 - \delta_5(\chi - \chi_1)) \chi \right]_{,\tau} = \\ \left[\chi_{,z} \Delta(\theta) \right]_{,z} + \delta_5 \left[\chi \theta_{,z} \left(\kappa(\theta) \theta_{,\tau} - \frac{3}{2} u_{,z} \sin^2 \theta \right) - \frac{1}{4} w_{,z} \sin 2\theta \right]_{,z}, \end{aligned} \quad (11)$$

where $\Delta(\theta) = \lambda \cos^2 \theta + \sin^2 \theta$, $\lambda = \lambda_{\parallel} / \lambda_{\perp}$, λ_{\parallel} and λ_{\perp} are the heat conductivity coefficients parallel and perpendicular to the director $\hat{\mathbf{n}}$, $\delta_4 = \rho_0 C_p K_{10} / (\gamma_{10} \lambda_{\perp})$ and $\delta_5 = T_{\text{NI}} K_{10} \xi / (\gamma_{10} \lambda_{\perp} d^2)$ are two extra parameters of the LC system. Note that the overbars in the space variable z , in the last four Eqs. (8)–(11) have also been eliminated.

Now the reorientation of the director in the HAN channel confined between two solid surfaces, when the relaxation regime is governed by the viscous, elastic, and thermomechanical forces, and with accounting for the flow, can be obtained by solving the system of the nonlinear partial differential Eqs. (7)–(11), with the appropriate boundary conditions for the polar angle (see Eqs. (4)), with the no-slip boundary condition for both velocities (see Eqs. (6)), and with the initial condition for the angle θ written in the form Eq. (5). Below we consider the case when the upper surface is hotter than the lower one, and the boundary condition for the temperature field must satisfy the Eq. (3).

For the case of 4-*n*-pentyl-4'-cyanobiphenyl (5CB), at temperature corresponding to nematic phase, the values of the material constants are borrowed from the Ref. [13]. Thus, the set of parameters values, which are involved in Eqs. (7)–(11) are: $\delta_1 \sim 0.3$, $\delta_2 \sim 24$, $\delta_3 \sim 2 \times 10^{-6}$, $\delta_4 \sim 6 \times 10^{-4}$, and $\delta_5 \sim 2 \times 10^{-9}$, respectively. Using the fact that $\delta_3 \ll 1$, the momentum balance equations (9) and (10) can be considerably simplified as velocities follows adiabatically the motion of the director. Thus, the whole left-hand side of Eqs. (9) and (10), can be neglected, reducing it to

$$\sigma_{zx} = h(\theta) u_{,z} - \mathcal{A}(\theta) \theta_{,\tau} - \delta_2 \chi_{,z} \theta_{,z} \sin^2 \theta + \frac{\beta_0}{6} w_{,z} \sin 2\theta = C_1(\tau), \quad (12)$$

and

$$\sigma_{zz} = \frac{\beta_0}{6} \left(u_{,z} \sin 2\theta + \frac{2}{3} w_{,z} \right) - \frac{\delta_2}{4} \chi_{,z} \theta_{,z} \sin 2\theta - \mathcal{G}(\theta) \theta_{,z}^2 = C_2(\tau), \quad (13)$$

respectively, where the functions $C_1(\tau)$ and $C_2(\tau)$ does not depends on z and will be fixed by the boundary conditions. Eq. (11) also can be considerably simplified, because both parameters δ_4 , $\delta_5 \ll 1$, and the whole left-hand side of Eq. (11), as well as the second term, can be neglected, so that Eq. (11) takes a form

$$\left[\chi_{,z} \Delta(\theta) \right]_{,z} = \left[\chi_{,z} (\lambda \cos^2 \theta + \sin^2 \theta) \right]_{,z} = 0. \quad (14)$$

The last equation has a solution

$$\chi(z, \tau) = \frac{\Delta \chi}{I} \int_0^z (\lambda \cos^2 \theta + \sin^2 \theta)^{-1} dz + \chi_i, \quad (15)$$

where $I = \int_0^1 (\lambda \cos^2 \theta + \sin^2 \theta)^{-1} dz$, $\Delta \chi = \chi_2 - \chi_1$, and $\chi_i = T_i / T_{\text{NI}}$, respectively.

3. Effect of thermomechanical force on relaxation processes in compressible nematic fluids

In case of the micro-sized (a few microliters) HAN channel confined between two horizontal surfaces and heated from below the hydrodynamic flow \mathbf{v} is excited in the nematic volume. The thermomechanical contribution σ^{tm} to the value of \mathbf{v} excited by $\nabla\chi$ in the hybrid aligned nematic channel with the thickness d is proportional to

$$u \sim \frac{d}{\eta} \sigma_{zx}^{\text{tm}} \sim -\frac{d}{\eta} \delta_2 \chi_{,z} \theta_{,z} \sin^2 \theta,$$

for the horizontal component of velocity (see also Eq. (12)), while the same contribution to the vertical component of velocity is equal to

$$w \sim \frac{d}{\eta} \sigma_{zz}^{\text{tm}} \sim -\frac{d}{4\eta} \delta_2 \chi_{,z} \theta_{,z} \sin 2\theta,$$

(see also Eq. (13)), respectively. Here η is the viscosity, and σ_{zx}^{tm} and σ_{zz}^{tm} are the shear and normal components of the thermomechanical contribution to the full stress tensor.

It should be noted that the additional effect of the thermomechanical force, due to ξ or δ_2 , on the velocity \mathbf{v} occurs due to the dependence both of θ and χ on δ_2 , as shown in Eqs. (8) and (15). Indeed, the effect of the thermomechanical force on the evolution of the polar angle θ is proportional $-\delta_2 \chi_{,z} \theta_{,z} \kappa(\theta)$.

In our previous simulations, ξ was estimated as 10^{-12} J/m K [13], and the dimensionless parameter $\delta_2 = \xi T_{NI}/K_{10}$ which reflects the effect of the thermomechanical force on the relaxation in a micro-sized nematic volume was equal to 24 [13]. Now we will expand our calculations to two values of δ_2 , the first of which is 20, and the second is 40. The evolution of the director, velocity and temperature fields during of our numerical study has been obtained by solving nonlinear partial differential equations (8), (12), (13) and (15), together with the boundary conditions (3), (4) and (6), and with the initial condition (5) by the numerical relaxation method [17]. In the calculations, the relaxation criterion $\epsilon = |\theta_{(m+1)}(z, \tau) - \theta_{(m)}(z, \tau)|/\theta_{(m+1)}(z, \tau)$ was chosen to be equal to 10^{-4} , and the numerical procedure was then carried out until a prescribed accuracy was achieved. Here m is the iteration number and τ_R is the relaxation time.

First of all, we will study the effect of the thermomechanical force on the relaxation of the polar angle $\theta(z, \tau_i)$ ($i = 1, \dots, 5$) as a function of the dimensionless distance z counted from the lower cooler $\chi_{z=0} = \chi_1$ to the upper warmer $\chi_{z=1.0} = \chi_1 + \Delta\chi$ (CASE I) bounding surface, for the compressible nematic film. It should be noted that ξ , or δ_2 is included in the torques and linear momentum balance equations (see, Eqs. (8), (12), and (13)), respectively. Relaxation of the polar angle $\theta(z, \tau_i)$ ($i = 1, \dots, 5$) as a function of the dimensionless distance z , during the first 5 time terms (τ_i ($i = 1, \dots, 5$)) and for $\delta_2 = 20$ (see Fig. 2(a)) and $\delta_2 = 40$ (see Fig. 2(b)) is shown in Fig. 2. Here the number of dimensionless times τ_i increases from curve (1) to curve (5), while $\chi_1 = 0.97$, $\Delta\chi = 0.0162$ and $\tau_0 = 0.1$, respectively. Results of calculation show that during the first 5 time term (from τ_1 to τ_5), changes in the distribution of polar angle across the LC sample are very similar and characterized by a set of convex curves. In case of $\delta_2 = 20$, z -dependence of the polar angle is characterized by an almost linear increase in the value of $\theta(z, \tau_5)$ from 0 to $\pi/2$, while in case of $\delta_2 = 40$, the same dependence is characterized by a convex curve that saturates after $z \sim 0.8$ and is equal to $\pi/2$. The relaxation of the dimensionless temperature $\chi(z, \tau_i)$ ($i = 1, \dots, 5$) as a function of the dimensionless distance z counted from the lower cooler $\chi_{z=0} = \chi_1$ to the upper warmer $\chi_{z=1.0} = \chi_1 + \Delta\chi$ (CASE I) bounding surface, for the compressible nematic film, during the first 5 time terms (τ_i ($i = 1, \dots, 5$)) and for $\delta_2 = 20$ (see Fig. 3(a)) and $\delta_2 = 40$ (see Fig. 3(b)) is shown in Fig. 3. Results of calculation show that during the first 5 time term (from τ_1 to τ_5), changes in the distribution of temperature $\chi(z, \tau_i)$ ($i = 1, \dots, 5$) across the LC sample are very similar and are characterized by a set of slightly concave curves.

As can be seen from Fig. 4, δ_2 has an even more significant effect on the evolution of horizontal component of velocity $u(z, \tau_i)$ ($i = 1, \dots, 5$). Here the values of dimensionless times $\tau_i = \tau_0 i$, ($i = 1, \dots, 8$) are the same as in Fig. 2. Analysis of the shear ST component σ_{zx} (see Eq. (12)) shows that the main contribution to the value of u is due to the thermomechanical force $-\delta_2 \chi_{,z} \theta_{,z} \sin^2 \theta$. In both cases of δ_2 , equal to 20 and 40, this contribution is negative. It should be noted that during the first 5 time terms (from τ_1 to τ_5), both distributions of the horizontal component of velocity $u(z, \tau_i)$ ($i = 1, \dots, 5$) as a function of the dimensionless distance z are similar and characterized by a decrease in the local maximum values. In case $\delta_2 = 20$, this distribution is characterized by decrease of the local maximum near the cooler lower boundary from $|u(z = 0.12, \tau_1)| \sim 4.7$ to $|u(z = 0.27, \tau_5)| \sim 2.0$, directed in the negative direction, while in case of $\delta_2 = 40$, this distribution is characterized by decrease the local maximum also near the cooler lower boundary from $|u(z = 0.17, \tau_1)| \sim 25.6$ to $|u(z = 0.46, \tau_5)| \sim 3.2$, directed in the negative direction. Thus, in both these cases, due to the balance of forces acting per unit LC volume, in which the thermomechanical contribution prevails, a hydrodynamic flow is formed in the negative direction.

It should be noted that with growth of ξ or δ_2 , in two times, from $\delta_2 = 20$ to $\delta_2 = 40$, the maximum value of the horizontal component of velocity, after 5 time terms, increases from $|u(\delta_2 = 20)| \sim 2.0$ to $|u(\delta_2 = 40)| \sim 3.2$, respectively.

Finally, the evolution of $w - u$ diagram for the case of lower cooler ($\chi_{z=0} = \chi_1$) and upper hotter ($\chi_{z=1} = \chi_1 + \Delta\chi$) bounding surfaces (CASE I), and for the number of dimensionless times $\tau_i = \tau_0 i$, ($i = 1, \dots, 5$), whose values increase from curve (1) to curve (5), but for differ value of $\delta_2 = 20$ (see Fig. 5(a)) and $\delta_2 = 40$ (see Fig. 5(b)) is shown in Fig. 5. Here $\chi_1 = 0.97$, $\Delta\chi = 0.0162$ and $\tau_0 = 0.1$, respectively. This behavior is characterized by a monotonic decreasing in the absolute values of both velocity components u and w , with the vertical component of the velocity directed in the positive direction, while the horizontal component is directed in the negative direction.

4. Formulation of the balance equations for incompressible nematic fluids

In the following we would like to carried out the comparative analysis of the relaxation regimes of the formation of hydrodynamic flow caused by thermomechanical force in both compressible and incompressible HAN microvolume. As a first step, we need to reformulate the basic hydrodynamic equations, taking into account some of the features characteristic of the incompressible nematic fluid. Since we are dealing with the complex flow $\mathbf{v}(z, \tau)$ excited by the temperature gradient and the director reorientation, the incompressibility condition $\nabla \cdot \mathbf{v} = 0$ implies that only one nonzero component of the vector \mathbf{v} exists, and the velocity it has only the horizontal component, viz. $\mathbf{v}(z, \tau) = v_x(z, \tau) \hat{\mathbf{i}} = u(z, \tau) \hat{\mathbf{i}}$.

In case of an incompressible nematic the dimensionless torque balance equation describing the reorientation of the LC phase can be written as

$$\gamma_1(\chi)\theta_{,\tau} = \mathcal{A}(\theta)u_{,z} + (\mathcal{G}(\theta)\theta_{,z})_{,z} - \frac{1}{2}\mathcal{G}_{,\theta}(\theta)\theta_{,z}^2 - \delta_2\chi_{,z}\theta_{,z}, \quad (16)$$

while the balance of dimensionless impulses acting per unit LC volume reduces to

$$\delta_3 u_{,\tau} = [h(\theta)u_{,z} - \mathcal{A}(\theta)\theta_{,\tau} - \delta_2\chi_{,z}\theta_{,z}\sin^2\theta]_{,z}, \quad (17)$$

respectively.

Using the fact that $\delta_3 \ll 1$, Eq. (17) can be considerably simplified as velocities follows adiabatically the motion of the director. Thus, the whole left-hand side of Eq. (17), can be neglected, reducing it to

$$\sigma_{zx} = h(\theta)u_{,z} - \mathcal{A}(\theta)\theta_{,\tau} - \delta_2\chi_{,z}\theta_{,z}\sin^2\theta = C_3(\tau), \quad (18)$$

where the function $C_3(\tau)$ does not depends on z and will be fixed by the boundary conditions.

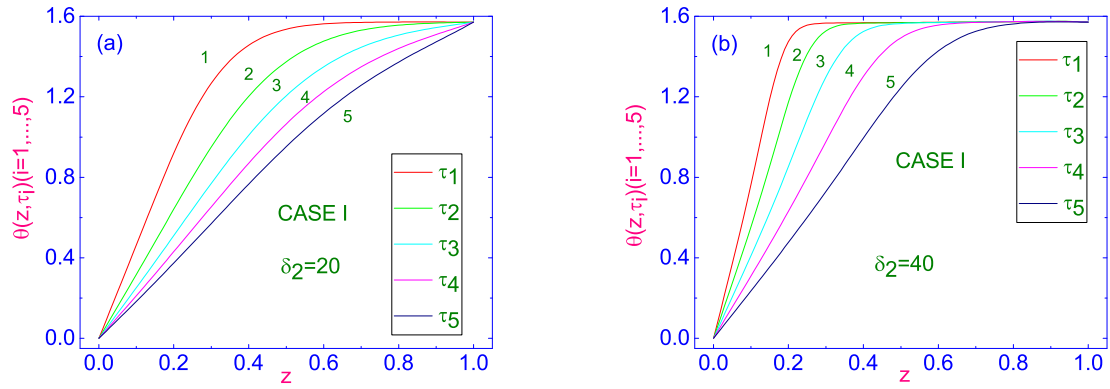


Fig. 2. (a) The polar angle $\theta(z, \tau_i)$ ($i = 1, \dots, 5$) as a function of the dimensionless distance z counted from the lower cooler $\chi_{z=0} = \chi_1$ to the upper warmer $\chi_{z=1.0} = \chi_1 + \Delta\chi$ (CASE I) bounding surface, for the compressible nematic film. In both cases (a) and (b), the dimensionless parameter δ_2 is equal to 20 and 40, respectively. Here the number of dimensionless times $\tau_i = \tau_0 i$, ($i = 1, \dots, 5$), whose values increase from curve (1) to curve (5), while $\chi_1 = 0.97$, $\Delta\chi = 0.0162$ and $\tau_0 = 0.1$, respectively.

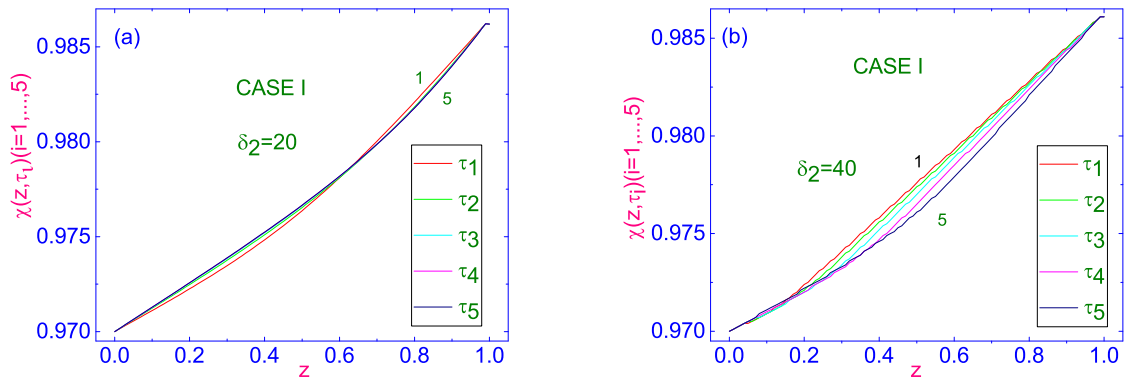


Fig. 3. Same as in Fig. 2, but for the dimensionless temperature $\chi(z, \tau_i)$ ($i = 1, \dots, 5$) as a function of the dimensionless distance z and a number of dimensionless times $\tau_i = \tau_0 i$, ($i = 1, \dots, 5$).

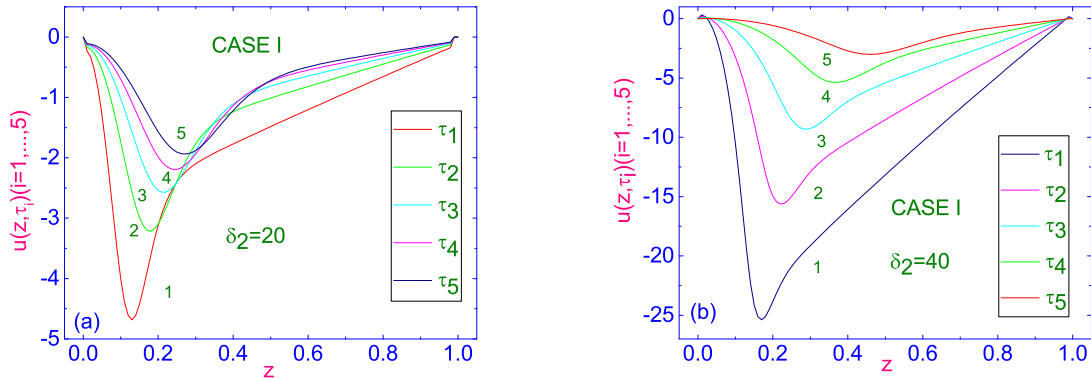


Fig. 4. The horizontal component of velocity $u(z, \tau_i)$ ($i = 1, \dots, 8$) as a function of the dimensionless distance z counted from the lower cooler $\chi_{z=0} = \chi_1$ to the upper warmer $\chi_{z=1} = \chi_1 + \Delta\chi$ (CASE I) bounding surface, for compressible nematic film. In case (a) the dimensionless parameter δ_2 is equal to 20, while in case (b), is equal to 40, respectively.

When the small temperature gradient $\nabla\chi$ is set up across the incompressible HAN channel, we expect that the temperature field $\chi(z, t)$ satisfies the dimensionless heat conduction equation

$$\delta_4 \chi_{,t} = [\chi_{,z} \Delta(\theta)]_{,z} + \delta_5 \left[\chi \theta_{,z} \left(\kappa(\theta) \theta_{,z} - \frac{3}{2} u_{,z} \sin^2 \theta \right) \right]_{,z}. \quad (19)$$

Eq. (19) can also be considerably simplified, since both parameters δ_4 , $\delta_5 \ll 1$, so the Eq. (19) takes the form of Eq. (15).

Now the reorientation of the director in the incompressible HAN channel confined between two solid surfaces, when the relaxation regime is governed by the viscous, elastic, and thermomechanical

forces, and with accounting for the flow, can be obtained by solving the system of the nonlinear partial differential Eqs. (16), (18) and (15), with the appropriate boundary conditions, both for the polar angle θ (see Eq. (4)) and no-slip boundary condition for the horizontal component $u(z)$ of velocity (see Eq. (6)), while the boundary condition for the temperature field is chosen in case I (see Eq. (3)).

Calculations of evolution of the director \hat{n} to its equilibrium orientation \hat{n}_{eq} , which is described by the polar angle $\theta(\chi, \tau)$, from the initial condition $\theta(z, \tau = 0) = \frac{\pi}{2} z$ to θ_{eq} , both for the compressible (Fig. 6(a)) and incompressible (Fig. 6(b)) nematic channels, and for the number

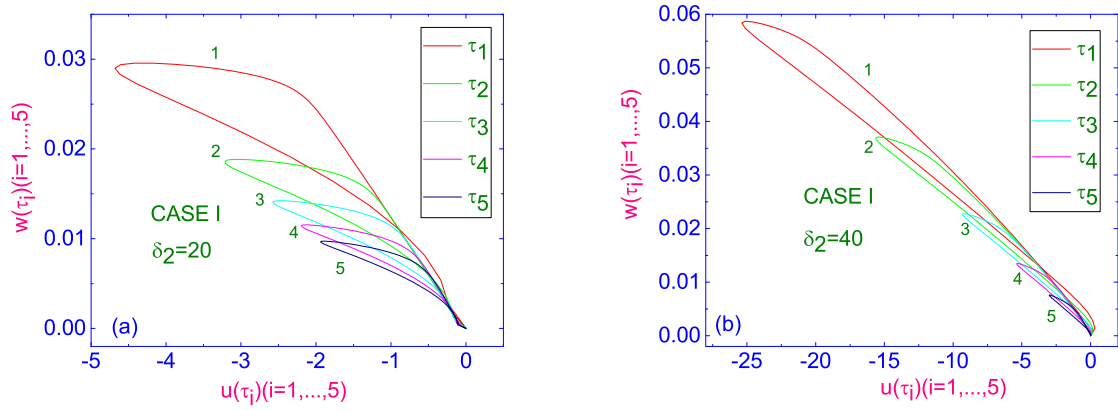


Fig. 5. (a) Evolution of $w-u$ diagram for the case of lower cooler ($\chi_{z=0} = \chi_1$) and upper hotter ($\chi_{z=1} = \chi_1 + \Delta\chi$) bounding surfaces (CASE I), and for the number of dimensionless times $\tau_i = \tau_0 i$, ($i = 1, \dots, 5$), whose values increase from curve (1) to curve (5). Here $\chi_1 = 0.97$, $\Delta\chi = 0.0162$ and $\tau_0 = 0.1$, respectively. (b) Same as in (a), but for $\delta_2 = 40$.

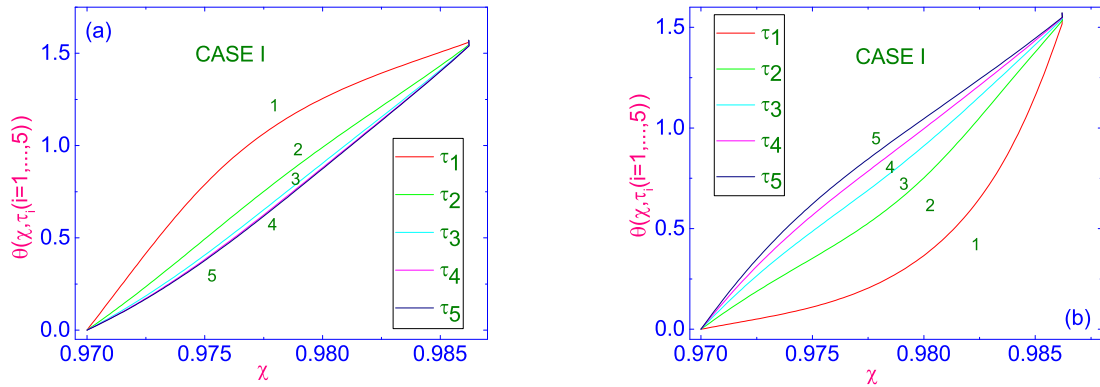


Fig. 6. Temperature dependence of polar angle $\theta(\chi, \tau_i)$ ($i = 1, \dots, 5$), both for the compressible (a) and incompressible (b) nematic films, and for the number of dimensionless times $\tau_i = \tau_0 i$, ($i = 1, \dots, 5$), whose values increase from curve (1) to curve (5). In these cases (a) and (b), the values of the temperature on both bounding surfaces are: $\chi_{z=0} = \chi_1$, $\chi_{z=1.0} = \chi_1 + \Delta\chi$ (CASE I), respectively. Here $\chi_1 = 0.97$, $\Delta\chi = 0.0162$ and $\tau_0 = 0.1$.

of dimensionless times $\tau_i = \tau_0 i$, ($i = 1, \dots, 5$), whose values increase from curve (1) to curve (5), are shown in Fig. 6. It should be noted that both of these dependencies are calculated for case I, when the value of the temperature on both bounding surfaces are: $\chi_{z=0} = \chi_1$, $\chi_{z=1.0} = \chi_1 + \Delta\chi$ (CASE I), while $\chi_1 = 0.97$, $\Delta\chi = 0.0162$ and $\tau_0 = 0.1$, respectively. In case of compressible HAN sample, when the LC sample is heated from above with the dimensionless temperature difference $\Delta\chi = 0.0162$ (~ 5 K), the profiles of the polar angle $\theta(\chi, \tau_i)$ ($i = 1, \dots, 5$) are characterized by monotonic transformation from convex (see Fig. 6(a), first two curves $\theta(\chi, \tau_i)$ ($i = 1, 2$)) to concave (see Fig. 6(a), the last three $\theta(\chi, \tau_i)$ ($i = 3, \dots, 5$)) curves, while in case of incompressible HAN sample, the evolution of these profiles of polar angle $\theta(\chi, \tau_i)$ ($i = 1, \dots, 5$) are characterized by monotonic transformation from concave (see Fig. 5(b), first two curves $\theta(\chi, \tau_i)$ ($i = 1, 2$)) to concave (see Fig. 6(b), the last three curves $\theta(\chi, \tau_i)$ ($i = 3, \dots, 5$)), respectively. These distinguishes in the equilibrium distribution of the angle $\theta(\chi, \tau_5)$ vs. temperature, for compressible and incompressible cases finally influences on distributions of the horizontal component of velocity. The dependencies of $u(z, \tau_i)$ ($i = 1, \dots, 5$) as a function of the dimensionless distance z counted from the lower cooler $\chi_{z=0} = \chi_1$ to the upper warmer $\chi_{z=1.0} = \chi_1 + \Delta\chi$ bounding surfaces are shown in Fig. 7(a) and (b). If the maximum values of $|u_{eq}(z = 0.27)| = 1.93$ (compressible HAN) and $|u_{eq}(z = 0.98)| = 3.13$ (incompressible HAN) are relatively close, the shapes of these distributions differ sufficiently.

This behavior of the horizontal velocity component $u(z, \tau_i)$ ($i = 1, \dots, 5$), depending on the dimensionless distance z for both compressible and incompressible nematic films, is due to the different

evolution of the profiles of the polar angle $\theta(\chi, \tau_i)$, and the temperature $\chi(\tau_i)$ ($i = 1, \dots, 5$) across the HAN sample. Thus, a small quantitative difference was found in the equilibrium distribution of the horizontal velocity component for both compressible and incompressible nematic flow caused by the same temperature gradient, which is set up across the micro-sized LC channel.

5. Conclusion

In summary, we conducted the numerical study of the effect of thermomechanical force on dissipation processes in a micro-sized compressible and incompressible nematics under the influence of the same temperature gradient ∇T , which is set up across the micro-sized HAN channel. Our calculations, based upon the classical Leslie-Ericksen theory, with taking into account the entropy balance equation, show that the hybrid aligned compressible nematic sample under the effect of ∇T , directed from the lower cooler to upper hotter bounding surfaces, settles down to a stationary flow regime with the horizontal u and vertical w components of velocity. We investigated the effect of thermomechanical force on relaxation processes in compressible nematic liquids and found that with an increase in this force, not only the magnitude of the horizontal velocity component increases, but can observe also the change of the director distribution across the HAN channel. A small quantitative difference was found in the equilibrium distribution of the horizontal velocity component for both compressible and incompressible nematic flow caused by the same ∇T .

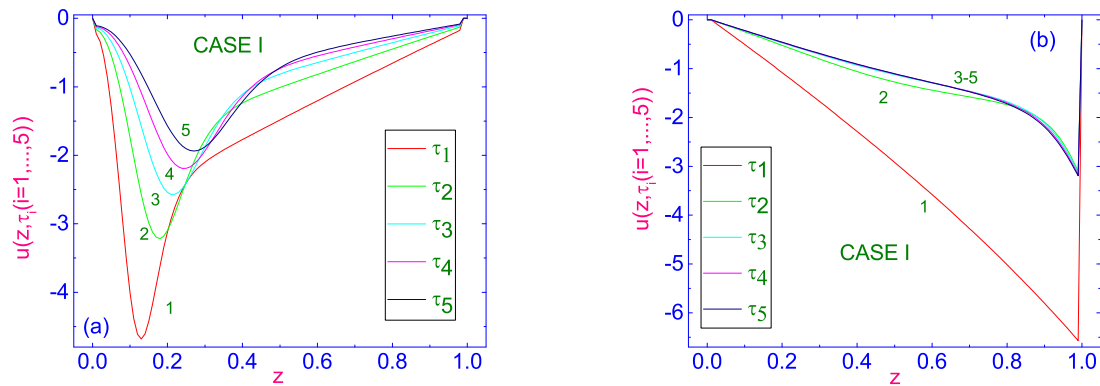


Fig. 7. The horizontal component of velocity $u(z, \tau_i)$ ($i = 1, \dots, 5$) as a function of the dimensionless distance z counted from the lower cooler $\chi_{z=0} = \chi_1$ to the upper warmer $\chi_{z=1.0} = \chi_1 + \Delta\chi$ (CASE I) bounding surface, for the compressible (a) and incompressible (b) HAN films. Here the number of dimensionless times $\tau_i = \tau_0 i$, ($i = 1, \dots, 5$), whose values increase from curve (1) to curve (5), while $\chi_1 = 0.97$, $\Delta\chi = 0.0162$ and $\tau_0 = 0.1$, respectively.

We believe that the present study may shed some light on the problem of the reorientation process in a compressible nematic channel under the influence of a vertical temperature gradient. We also believe that the paper shows not only some useful routes for estimation of the relaxation times, but also for analyzing the remaining problems associated with LC's device stability, efficiency, and lifetime.

CRediT authorship contribution statement

Izabela Šliwa: Investigation, Conceptualization. **Pavel V. Maslennikov:** Investigation. **Sergey V. Pasechnik:** Validation, Formal analysis. **Alex V. Zakharov:** Writing – review & editing, Writing – original draft, Supervision, Investigation, Conceptualization.

Declaration of competing interest

The authors have no conflicts to disclose

Acknowledgments

A. V. Z. acknowledges financial support of the Fundamental Research Program of the National Research University Higher School of Economics, Russia (FR-2025-75).

Data availability

No data was used for the research described in the article.

References

- [1] O.O. Lehmann, Ann. Phys. (Leipzig) 4 (1900) 649.
- [2] R.S. Akopyan, B.Ya. Zeldovich, Sov. Phys. JETP 60 (1984) 953.
- [3] R.S. Hokobyan, G.L. Yesayan, B.Ya. Zeldovich, Phys. Rev. E 73 (2006) 061701.
- [4] A.V. Zakharov, A.A. Vakulenko, J. Chem. Phys. 127 (2007) 084907.
- [5] E. Varneuil, M.L. Cordero, F. Gallaire, Ch. Baroud, Langmuir 25 (2009) 5127.
- [6] M.L. Cordero, E. Verneuil, F. Gallaire, Ch. Baroud, Phys. Rev. E 79 (2009) 011201.
- [7] A.V. Zakharov, A.A. Vakulenko, M. Iwamoto, J. Chem. Phys. 132 (2010) 224906.
- [8] A.V. Zakharov, A.A. Vakulenko, Phys. Fluids 27 (2015) 062001.
- [9] H. Choi, H. Takezoe, Soft Matter 12 (2016) 481.
- [10] A.V. Zakharov, P.V. Maslennikov, Phys. Rev. E 96 (2017) 052705.
- [11] I. Šliwa, A.V. Zakharov, Symmetry 13 (2013) 459.
- [12] I. Šliwa, P.V. Maslennikov, D.P. Shcherbinin, A.V. Zakharov, Phys. Rev. E 110 (2024) 064702.
- [13] I. Šliwa, P.V. Maslennikov, A.V. Zakharov, Crystals 15 (2025) 235.
- [14] J.L. Ericksen, Arch. Ration. Mech. Anal. 4 (1960) 231.
- [15] F.M. Leslie, Arch. Ration. Mech. Anal. 28 (1968) 265.
- [16] L.D. Landau, E.M.E.M. Lifshitz, Fluid Mechanics, Pergamon, Oxford, 1987.
- [17] I.S. Berezin, N.P. Zhidkov, Computing Methods, fourth ed., Pergamon Press, Oxford, 1965.